



## ISHT MEETING

# Restoring discarded porcine lungs by ex vivo removal of neutrophil extracellular traps

Margareta Mittendorfer, MSc,<sup>a,b,c,d</sup> Leif Pierre, PhD,<sup>b,c,d</sup> Tibor Huzevka, MD,<sup>a,b,c,d</sup> Jeremy Schofield, MD,<sup>e</sup> Simon T. Abrams, PhD,<sup>e</sup> Guozheng Wang, PhD,<sup>e</sup> Cheng-Hock Toh, MD, PhD,<sup>e,f</sup> Nicholas B. Bèchet, PhD,<sup>a,b,c,d</sup> Ilma Caprnja, MD,<sup>a,b,c,d</sup> Gunilla Kjellberg, PhD,<sup>g</sup> Andrew Aswani, MD, PhD,<sup>h,i</sup> Franziska Olm, PhD,<sup>a,b,c,d</sup> and Sandra Lindstedt, MD, PhD<sup>a,b,c,d</sup>

From the <sup>a</sup>Department of Clinical Sciences, Lund University, Lund, Sweden; <sup>b</sup>Department of Cardiothoracic Surgery and Transplantation, Lund University Hospital, Lund, Sweden; <sup>c</sup>Wallenberg Centre for Molecular Medicine, Lund University, Lund, Sweden; <sup>d</sup>Lund Stem Cell Centre, Lund University, Lund, Sweden; <sup>e</sup>Department of Clinical Infection, Microbiology and Immunology, University of Liverpool, Liverpool, United Kingdom; <sup>f</sup>Roald Dahl Haemostasis & Thrombosis Centre, Liverpool University Hospitals NHS Foundation Trust, Liverpool, United Kingdom; <sup>g</sup>Department of Thoracic Surgery and Anaesthesiology, Uppsala University Hospital, Uppsala, Sweden; <sup>h</sup>Department of Critical Care, Guy's and St Thomas's NHS Foundation Trust, London, United Kingdom; and the <sup>i</sup>Santerus AG, Zurich, Switzerland.

**KEYWORDS:**

lung transplantation;  
EVLP;  
NETs;  
gastric aspiration;  
donor

**BACKGROUND:** By causing inflammation and tissue damage, neutrophil extracellular traps (NETs) constitute an underlying mechanism of aspiration-induced lung injury, a major factor of the low utilization of donor lungs in lung transplantation (LTx).

**METHODS:** To determine whether NET removal during ex vivo lung perfusion (EVLP) can restore lung function and morphology in aspiration-damaged lungs, gastric aspiration lung injury was induced in 12 pigs. After confirmation of acute respiratory distress syndrome, the lungs were explanted and assigned to NET removal connected to EVLP (treated) ( $n = 6$ ) or EVLP only (nontreated) ( $n = 6$ ). Hemodynamic measurements were taken, and blood and tissue samples were collected to assess lung function, morphology, levels of cell-free DNA, extracellular histones, and nucleosomes as markers of NETs, as well as cytokine levels.

**RESULTS:** After EVLP and NET removal in porcine lungs, PaO<sub>2</sub>/FiO<sub>2</sub> ratios increased significantly compared to those undergoing EVLP alone ( $p = 0.0411$ ). Treated lungs had lower cell-free DNA ( $p = 0.0260$ ) and lower levels of extracellular histones in EVLP perfusate ( $p = 0.0260$ ) than nontreated lungs. According to histopathology, treated lungs showed less immune cell infiltration and less edema compared with nontreated lungs, which was reflected in decreased levels of proinflammatory cytokines in EVLP perfusate and bronchoalveolar lavage fluid.

**CONCLUSIONS:** To conclude, removing NETs during EVLP improved lung function and morphology in aspiration-damaged donor lungs. The ability to remove NETs during EVLP could represent a new therapeutic approach for LTx and potentially expand the donor pool for transplantation.

J Heart Lung Transplant xxxx;xxx:xxx-xxx

© 2024 The Authors. Published by Elsevier Inc. on behalf of International Society for Heart and Lung Transplantation. This is an open access article under the CC BY license (<http://creativecommons.org/licenses/by/4.0/>).

Reprint requests: Sandra Lindstedt, Department of Cardiothoracic Surgery and Transplantation, Skåne University Hospital, SE-221 85 Lund, Sweden.  
E-mail address: [sandra.lindstedt@med.lu.se](mailto:sandra.lindstedt@med.lu.se).

Lung transplantation (LTx) is an established therapeutic option for end-stage pulmonary disease. Yet its full clinical application remains hindered by a scarcity of organs. LTx outcome is inferior compared to other solid organ transplants with a 5-year survival rate of <65%.<sup>1,2</sup> Despite improvements in the procedure, primary graft dysfunction (PGD) remains the leading cause of early mortality, and rejection persists as the leading cause of late mortality. Fear of these complications leads to low utilization (approximately 20%) of donated lungs.<sup>3,4</sup>

Aspiration of gastric contents is a serious complication that can occur in organ donors, leading to acute lung injury (ALI).<sup>5</sup> Most potential donor lungs are discarded based on graft quality concerns due to ALI sustained before organ retrieval, such as neurogenic edema secondary to brain injury but also infection and gastric aspiration.<sup>6</sup> Currently, there are no options for treating discarded donor lungs to render them suitable for LTx. Treatments that restore or regenerate declined donor lungs should be explored to combat waiting list mortality.<sup>7</sup>

One of the mechanisms underlying aspiration-induced lung injury is the formation of neutrophil extracellular traps (NETs).<sup>8-10</sup> These inflammatory net-like structures comprise chromatin, histones, and granular proteins, released by activated neutrophils through NETosis.<sup>11-13</sup> NETs have been shown to cause tissue damage and inflammation, leading to injury and dysfunction of the lungs.<sup>14,15</sup> In the specific case of aspiration-induced ALI, NET levels corresponded with disease severity in murine models.<sup>8-10</sup>

Therapeutic targeting of NETs using DNase or other anti-NET therapies improved clinically relevant outcomes in various diseases and models, indicating that NET removal is a viable strategy for lung pathologies.<sup>8,16,17</sup> However, such therapies are associated with drawbacks, such as off-target effects and propagation of highly inflammatory fragmented NET components.<sup>13,18-20</sup> A novel approach to overcome those challenges is to selectively remove NETs from circulation, using an extracorporeal column containing histone-conjugated beads which avidly bind chromatin fragments.

Ex vivo lung perfusion (EVLP) involves the extracorporeal perfusion of lungs, which allows for pre-transplantation assessment and the possibility to selectively deliver therapeutic agents, thus emerging as a technique to expand the LTx donor pool.<sup>21-25</sup> Elevated levels of NETs in perfusate and post transplantation have been correlated with severe PGD post-LTx.<sup>26,27</sup>

We hypothesized that a NET removal device, connected to an EVLP circuit to remove NETs from the perfusate, ameliorates the inflammatory milieu in aspiration-damaged lungs to accelerate their recovery and improves function sufficiently to render them suitable for transplantation.

## Materials and methods

Additional details are described in the [Supplementary Materials](#).

## Ethical approval

Porcine experiments were approved by the Ethics Committee for Animal Research (Drn 5.2.18-4903/16 and Drn 5.2.18-8927/16).

## Animal preparation

Twelve Yorkshire pigs, both male and female (mean weight  $35 \pm 2$  kg), were assigned to receive EVLP alone (non-treated group,  $n = 6$ ) or EVLP in combination with a NET removal device (treated group,  $n = 6$ ). The animals were prepared as previously described.<sup>24</sup>

## Induction and establishment of aspiration-induced lung injury using gastric content

Gastric content, previously retrieved from pigs and stored at  $-80^{\circ}\text{C}$ , was mixed to homogeneity, centrifuged, and filtered (Fisher Scientific, Waltham, MA). All gastric content was titrated to pH 2 before instillation. The pigs were kept under anesthesia during the experiment. Mechanical ventilation was applied to the donor animals in the volume-controlled ventilation setting, with peak inspiratory pressure (PIP), respiratory rate, and fraction of inspired oxygen ( $\text{FiO}_2$ ) adjusted according to clinical demands. Following baseline measurements, each donor pig received 2 ml/kg/lung (total 4 ml/kg), distributed equally throughout the lung lobes via bronchoscopy, in 2 doses; the first dose contained 90% of the total gastric content, with the remaining 10% given 1 hour later. The following hemodynamic parameters were measured every 30 minutes by thermodilution with a Swan-Ganz catheter (Edwards Life Sciences, Irvine, CA) and arterial line (Merit Medical, Galway, Ireland): heart rate, systolic blood pressure, diastolic blood pressure, mean arterial pressure, cardiac index, systolic pulmonary pressure, diastolic pulmonary pressure, mean pulmonary pressure, pulmonary artery wedge pressure (Wedge), systemic vascular resistance, and pulmonary vascular resistance (PVR). A chest X-ray (CXR) was taken before administration of gastric content and hourly until organ harvest. Arterial blood gases were analyzed every 30 minutes with an ABL 90 FLEX blood gas analyzer (Radiometer Medical ApS, Brøndshøj, Denmark) before lung retrieval (during and after induction of acute respiratory distress syndrome [ARDS]).  $\text{PaO}_2/\text{FiO}_2$  ratios and CXR images were used to determine the induction of ARDS, which was retrospectively confirmed by histopathological analysis.

## EVLP of aspiration-injured lungs

Explanted lungs were subjected to EVLP per Ghaidan et al.<sup>24</sup>

## NET removal from porcine lungs

In the treated group, a NucleoCapture column (Santerus AG, Zürich, Switzerland<sup>28</sup>) which captures and removes NETs, nucleosomes, and other cell-free histones and DNA

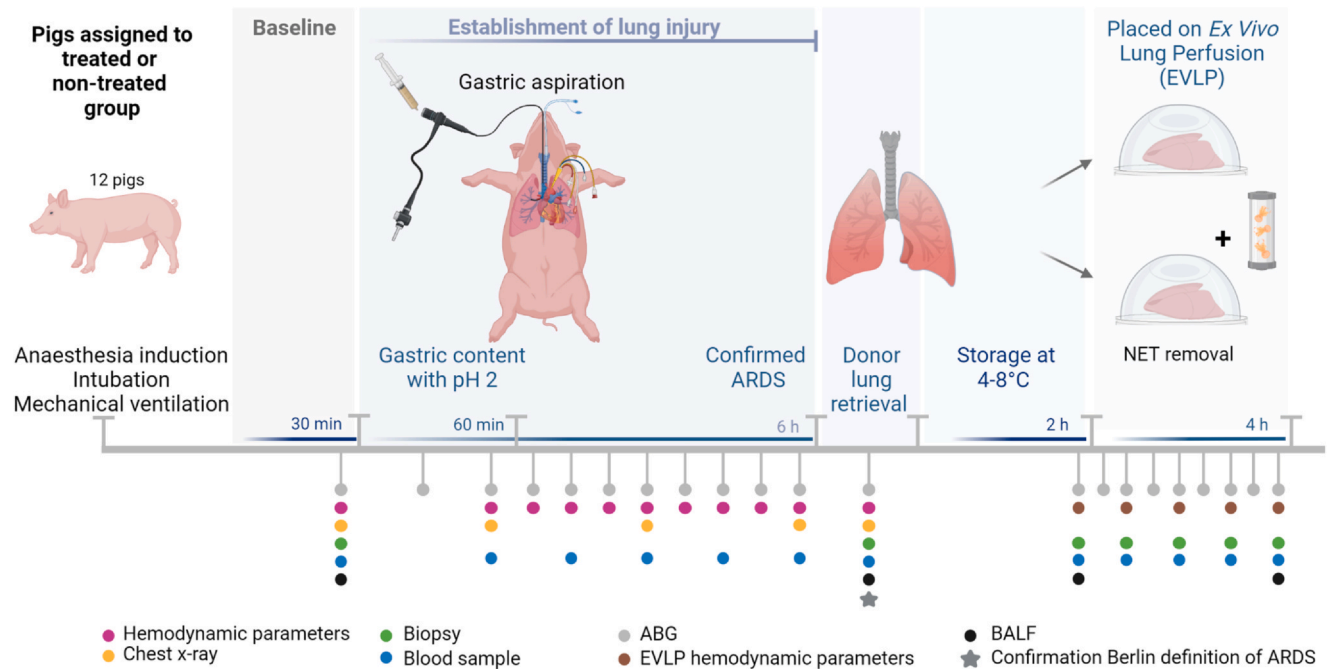


**Figure 1** Experimental overview and timeline. Twelve pigs were assigned to receive EVLP alone ( $n=6$ ) or EVLP and NET removal ( $n=6$ ). ARDS was induced by the instillation of gastric content with pH 2 into the lungs. Upon confirmation of ARDS, lungs were explanted and placed on EVLP with or without NET removal. Sampling intervals of hemodynamic parameters, chest X-rays, biopsies, blood samples, ABG, BALF, EVLP hemodynamic parameters, and the confirmation of ARDS are indicated. ABG, arterial blood gases; ARDS, acute respiratory distress syndrome; BALF, bronchoalveolar lavage fluid; EVLP, ex vivo lung perfusion; NET, neutrophil extracellular trap. Created with BioRender.com.

fragments, was connected to a Spectra Optia Apheresis System (perfusate flow 80 ml/min; Terumo BCT Inc., Terumo BCT Europe NV, Zaventem, Belgium), both of which were then placed in line with an EVLP circuit through a veno-venous shunt from the reservoir.

## Results

### Induction of ALI by intratracheal gastric content instillation

We first induced ARDS in all donor pigs through intratracheal delivery of gastric content. After confirmed ARDS, lungs were explanted, put in cold storage for 2 hours, and connected to EVLP (Figure 1). Donor animal hemodynamics, ventilatory settings, vitals, and blood gases are listed in Table 1. All animals experienced increases in PVR and PIP and decreased dynamic compliance ( $C_{dyn}$ ) on induction of lung injury, infiltrates on CXRs, decreased  $PaO_2/FiO_2$  ratio, and higher  $pCO_2$  (Figures 2A-2C, Table 1), confirming the development of ARDS. At the time of donor lung retrieval, there was no significant difference in  $PaO_2/FiO_2$  ratio between animals that were stratified to treatment ( $162.30 \pm 63.20$  mm Hg) or nontreatment groups ( $150.80 \pm 67.70$  mm Hg;  $p = 0.9372$ ; Figure 2A). At the time of lung retrieval, CXRs revealed bilateral infiltrates, in contrast to the X-rays before aspiration (baseline), which showed no visible infiltrates (Figure 2B). All pigs had established ARDS and significantly lower  $PaO_2/FiO_2$  ratios

versus baseline ( $156.60 \pm 62.70$  mm Hg vs  $505.30 \pm 58.56$  mm Hg;  $p = 0.0005$ , Figure 2C).

By histology, we observed intact alveolar barriers and open-air spaces in baseline lung tissue (Figure 2D, left), whereas lung injury was seen at the time of lung retrieval, evidenced by thickening of the alveolar walls, pulmonary edema, infiltration of immune cells into alveolar air spaces, and hemorrhage (Figure 2D, center). The overall lung injury score increased from  $0.04 \pm 0.01$  to  $0.81 \pm 0.03$  ( $p = 0.0022$ ) between baseline and retrieved lungs (Figure 2D, right) with scores being significantly elevated in all subcategories of scoring as well (Figure S1).

With regard to peripheral blood levels of NET-related markers, cell-free DNA was similar between baseline ( $253.3 \pm 81.28$  ng/ $\mu$ l) and time of confirmed ARDS ( $239.4 \pm 98.27$  ng/ $\mu$ l;  $p = 0.2189$ ; Figure 3A). Further, western blot analysis showed that total histone levels were higher, albeit insignificantly, from baseline ( $5.43 \pm 3.71$   $\mu$ g/ml) to confirmed ARDS ( $10.57 \pm 9.87$   $\mu$ g/ml,  $p = 0.1978$ ; Figure 3B, left). This increase was paralleled by a rise in H3 nucleosome levels from  $10.20 \pm 17.71$  ng/ml at baseline to  $19.25 \pm 16.10$  ng/ml at confirmed ARDS ( $p = 0.0205$ ; Figure 3B, right).

NET-specific histones were then analyzed by measuring citrullinated histone H3 (Cit-H3). Immunohistochemistry imaging scores for Cit-H3 (Figure 3C, left and middle) increased significantly ( $p = 0.0043$ ) from baseline ( $0.17 \pm 0.41$ ) to confirmed ARDS ( $2.50 \pm 0.84$ ). In contrast, extracellular Cit-H3 nucleosome levels in plasma remained unchanged at baseline ( $1.58 \pm 1.64$  ng/ml) to

**Table 1** Clinically Relevant Parameters for the Donor Lungs in the Treated and Nontreated Group, Documented Before Induction of ARDS, Termed Baseline, and at Confirmation of ARDS

Parameter	Baseline treated	Baseline nontreated	<i>p</i> value	Confirmed ARDS treated	Confirmed ARDS nontreated	<i>p</i> value
Sat (%)	99.83 ± 0.41	98.50 ± 1.52	0.1061	98.00 ± 3.16	95.33 ± 1.97	0.0649
HR (bpm)	94.83 ± 17.77	77.83 ± 4.66	0.0606	89.50 ± 17.07	76.00 ± 8.53	0.1039
MAP (mm Hg)	92.50 ± 15.33	86.83 ± 12.72	0.4610	86.17 ± 8.33	98.00 ± 8.22	0.0216
SPP (mm Hg)	26.50 ± 3.83	21.83 ± 2.86	0.0519	35.17 ± 4.26	35.00 ± 6.54	0.9048
DPP (mm Hg)	17.67 ± 3.01	12.50 ± 2.17	0.0087	22.17 ± 4.26	18.33 ± 4.46	0.1970
MPP (mm Hg)	21.67 ± 3.01	16.67 ± 2.66	0.0087	28.00 ± 4.19	24.67 ± 5.16	0.3723
PVR (DS/cm <sup>5</sup> )	238.00 ± 88.10	185.70 ± 31.60	0.3939	302.50 ± 82.30	368.30 ± 51.00	0.1320
CI (liter/min/m <sup>2</sup> )	3.01 ± 0.64	3.24 ± 0.61	0.6991	3.66 ± 0.49	2.59 ± 0.41	> 0.9999
pH	7.45 ± 0.07	7.44 ± 0.03	0.7857	7.42 ± 0.10	7.37 ± 0.05	0.3290
PaO <sub>2</sub> /FiO <sub>2</sub>	470.60 ± 45.20	540.00 ± 51.10	0.0411	162.30 ± 63.20	150.80 ± 67.70	0.9372
BE (mmol/liter)	4.67 ± 2.00	6.95 ± 2.20	0.1212	4.35 ± 2.46	4.90 ± 3.49	0.5130
Lactate (mmol/liter)	0.93 ± 0.56	0.92 ± 0.21	0.6710	1.10 ± 0.30	1.35 ± 0.69	0.5584
MV (liter/min)	7.02 ± 0.66	6.18 ± 1.02	0.1688	7.23 ± 0.47	6.92 ± 1.42	0.6688
PIP (cmH <sub>2</sub> O)	22.67 ± 2.58	16.8 ± 1.47	0.0043	27.33 ± 6.05	22.5 ± 3.99	0.1126
PEEP (cmH <sub>2</sub> O)	5.00 ± 0.00	5.00 ± 0.00	> 0.9999	5.00 ± 0.00	5.83 ± 1.16	0.1818
Vt (ml)	261.33 ± 15.59	273.83 ± 32.55	0.7879	265.17 ± 12.92	272.33 ± 39.79	0.5584
Cdyn (ml/cmH <sub>2</sub> O)	15.07 ± 2.30	23.45 ± 3.81	0.0022	12.51 ± 2.66	16.81 ± 3.27	0.0931
RR (breaths/min)	26.00 ± 1.09	21.80 ± 1.72	0.0022	27.17 ± 2.23	25.00 ± 4.52	0.4026

Abbreviations: ARDS, acute respiratory distress syndrome; BE, base excess, lactate (mmol/liter); Cdyn, dynamic compliance; CI, cardiac index; DPP, diastolic pulmonary pressure; HR, heart rate; MAP, mean arterial pressure; MPP, mean pulmonary pressure; MV, mechanical ventilator settings with volume-controlled ventilation: minute volume; PaO<sub>2</sub>/FiO<sub>2</sub>, blood gas parameters: pH, partial pressure of oxygen divided by fraction of inspired oxygen; PEEP, positive end-expiratory pressure; PIP, peak inspiratory pressure; PVR, pulmonary vascular resistance; RR, respiratory rate; Sat, oxygen saturation; SPP, hemodynamic variables: systolic pulmonary pressure; Temp, temperature; Vt, tidal volume.

The lungs later received either ex vivo lung perfusion and neutrophil extracellular trap removal (treated) or ex vivo lung perfusion only (nontreated).

All results are expressed as mean and standard deviation. Mann-Whitney tests were performed for statistical analysis. Statistical significance was defined as  $p \geq 0.05$  (not significant, ns),  $p < 0.05$  (\*),  $p < 0.01$  (\*\*).

confirmed ALI ( $1.56 \pm 2.08$  ng/ml,  $p = 0.8756$ ; [Figure 3C](#), right). Fibrin scores in tissue were similar between baseline and confirmed ARDS ( $1.83 \pm 0.75$  and  $2.50 \pm 0.84$ , respectively;  $p = 0.2100$ ; [Figure 3D](#)).

### Restoration of lung function and morphology following NET removal during EVLP

Following cold storage to mimic pretransplantation conditions, the explanted lungs underwent 4 hours of EVLP: 6 lungs with EVLP and NET removal (treated group) and 6 with EVLP alone (nontreated group). During EVLP, PIP, dynamic compliance, PVR and PAP remained constant, with no significant differences in these parameters between groups on completion of EVLP ([Figure 4A](#)). PaO<sub>2</sub>/FiO<sub>2</sub> ratios increased significantly after 4 hours in the treated ( $415.80 \pm 85.73$  mm Hg) versus nontreated group ( $275.40 \pm 120.30$  mm Hg,  $p = 0.0411$ ). Notably, 5 of 6 treated lungs had PaO<sub>2</sub>/FiO<sub>2</sub> ratios that exceeded 300 mm Hg, the clinical threshold of acceptability for transplantation, compared with 1 of 6 nontreated lungs ([Figure 4B](#)).

As a measure of edema in the lung, the wet-dry ratios of tissue biopsies from lungs of both groups were determined. As a result of NET removal, edema in treated lungs decreased, based on their lower wet-dry ratio ( $4.06 \pm 0.37$ ) versus nontreated grafts ( $4.99 \pm 0.57$ ;  $p = 0.0087$ ; [Figure 4C](#)).

By histology, treated lungs experienced significantly less infiltration, thickening of alveolar walls, and edema than

nontreated lungs, based on lung injury scores ( $0.21 \pm 0.06$  vs  $0.87 \pm 0.07$ , respectively;  $p = 0.0022$ ; [Figures 4D](#) and [S2](#)). Furthermore, the lungs in both groups showed decreased infiltration of immune cells compared with before EVLP ([Figure 4E](#), compared to [Figure 2D](#) center).

To determine whether the improved lung function and morphology resulted from the NET removal from the circulation, we analyzed NET-related elements in EVLP perfusate, lung tissue biopsies, and bronchoalveolar lavage fluid (BALF). Treated lungs had lower cell-free DNA levels in EVLP perfusate than nontreated lungs ( $781.50 \pm 230.30$  ng/μl vs  $1,599.00 \pm 981.60$  ng/μl;  $p = 0.0260$ , [Figure 5A](#)). Further, the levels of extracellular histones in EVLP perfusate were significantly lower by western blot analysis after NET removal ( $6.02 \pm 6.45$  μg/ml) versus nontreated lungs ( $19.02 \pm 7.51$  μg/ml;  $p = 0.0260$ , [Figure 5B](#)). However, H3 nucleosome content in perfusate was similar between groups ( $205.10 \pm 140.60$  ng/ml for treated and  $170.80 \pm 211.30$  ng/ml for nontreated, respectively;  $p = 0.4848$ , [Figure 5C](#)). With regard to NET-specific markers, the extracellular Cit-H3 nucleosome content in EVLP perfusate from treated animals was  $7.44 \pm 3.85$  ng/ml, compared with  $29.56 \pm 9.72$  ng/ml in the nontreated group ( $p = 0.0043$ , [Figure 5D](#)). To estimate the NET removal efficiency from the plasma, the ratio of Cit-H3 nucleosomes relative to total H3 nucleosomes was calculated. A significant difference between the treatment groups with a ratio of  $0.04 \pm 0.02$  in the treated group and a ratio of  $0.39 \pm 0.27$  in the nontreated group ( $p = 0.0087$ ,

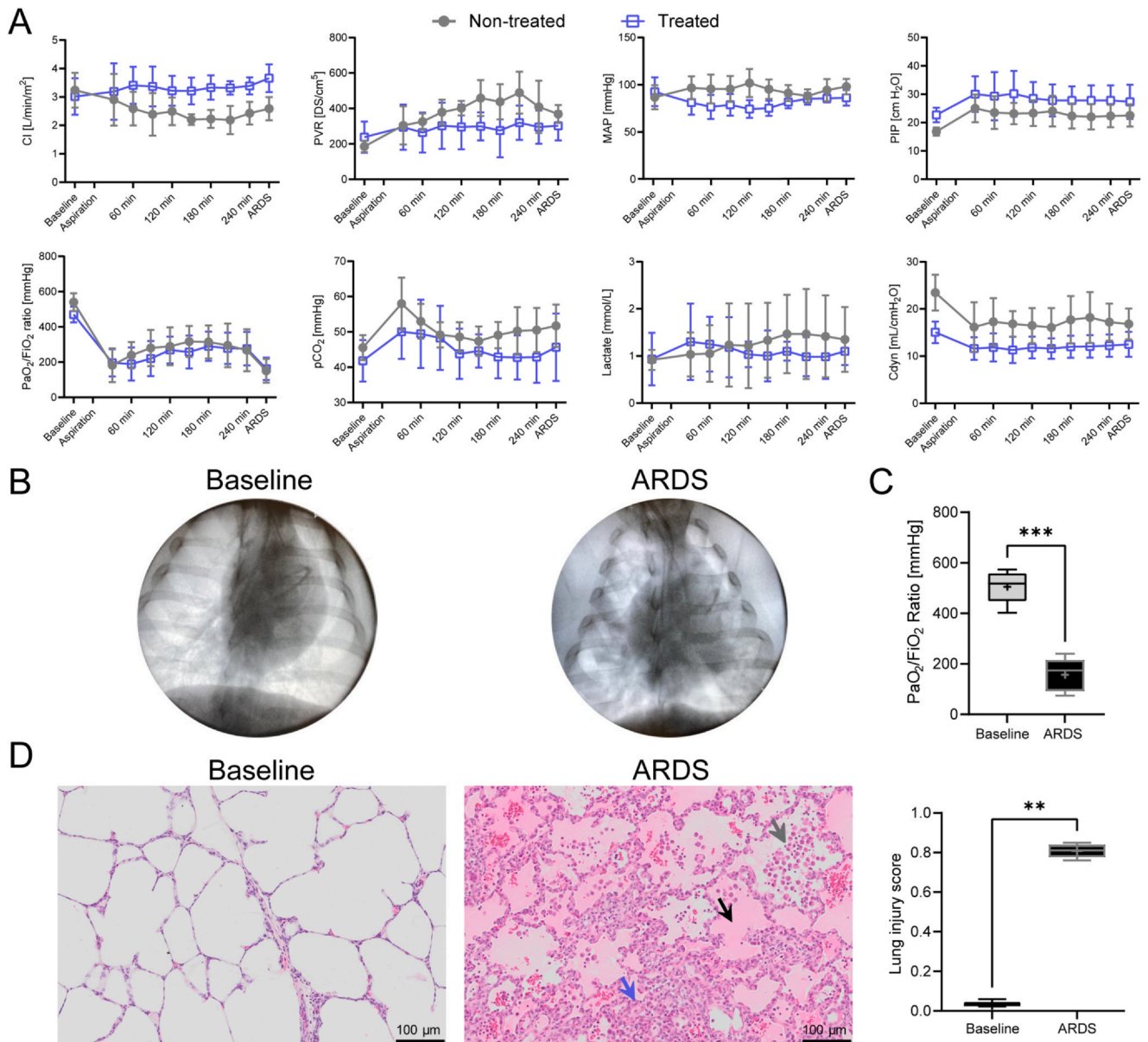


**Figure 2** Establishment of acute lung injury following gastric aspiration. (A) Selected hemodynamic and blood gas parameters for treated (blue squares) and nontreated lungs (gray full circles) over time from baseline (before instillation of gastric contents) until confirmation of ARDS, including cardiac index, pulmonary vascular resistance, mean arterial pressure, peak inspiratory pressure, PaO<sub>2</sub>/FiO<sub>2</sub> ratio, partial pressure of carbon dioxide, and dynamic compliance. Data are represented as mean ± SD. (B) Representative chest X-rays before induction of ARDS (baseline) and after ARDS was confirmed (ARDS). (C) PaO<sub>2</sub>/FiO<sub>2</sub> ratio in all pigs (n = 12) at baseline and after confirmation of ARDS. Statistical significance was tested with a 2-sided Wilcoxon test, \*\*\*p < 0.001. (D) Representative images of hematoxylin and eosin-stained histology sections of lung tissue at baseline (left) versus after confirmation of ARDS (middle), with arrows indicating thickening of alveolar walls (blue arrow), pulmonary edema (black arrow), and infiltration of immune cells into alveolar spaces (gray arrow). Scale bars represent 100 μm. Lung injury scores (right) comparing healthy lung tissue at baseline to tissue after ARDS was confirmed. Data are presented as boxplots with median lines, a plus at the mean, and whiskers indicating minimum and maximum. Statistical significance was tested with the 2-sided Mann-Whitney test, \*\*p < 0.01. ARDS, acute respiratory distress syndrome; Cdyn, dynamic compliance; CI, cardiac index; MAP, mean arterial pressure; pCO<sub>2</sub>, partial pressure of carbon dioxide; PIP, peak inspiratory pressure; PVR, pulmonary vascular resistance; SD, standard deviation.

Figure S3) was observed. Further, BALF from treated lungs had a lower concentration of extracellular Cit-H3 nucleosomes (480.10 ± 190.50 ng/ml) than nontreated lungs (3,480.00 ± 2,924.00 ng/ml; p = 0.0022; Figure 5E). Validating these ELISA results, Cit-H3 scores for lung tissue

stained by immunohistochemistry were significantly lower in the treated (0.00 ± 0.00) versus nontreated group (1.83 ± 0.98; p = 0.0022; Figure 5F). To examine the effects of NET removal on fibrin deposition in ARDS, we analyzed fibrin content in lung tissue by immunohistochemistry

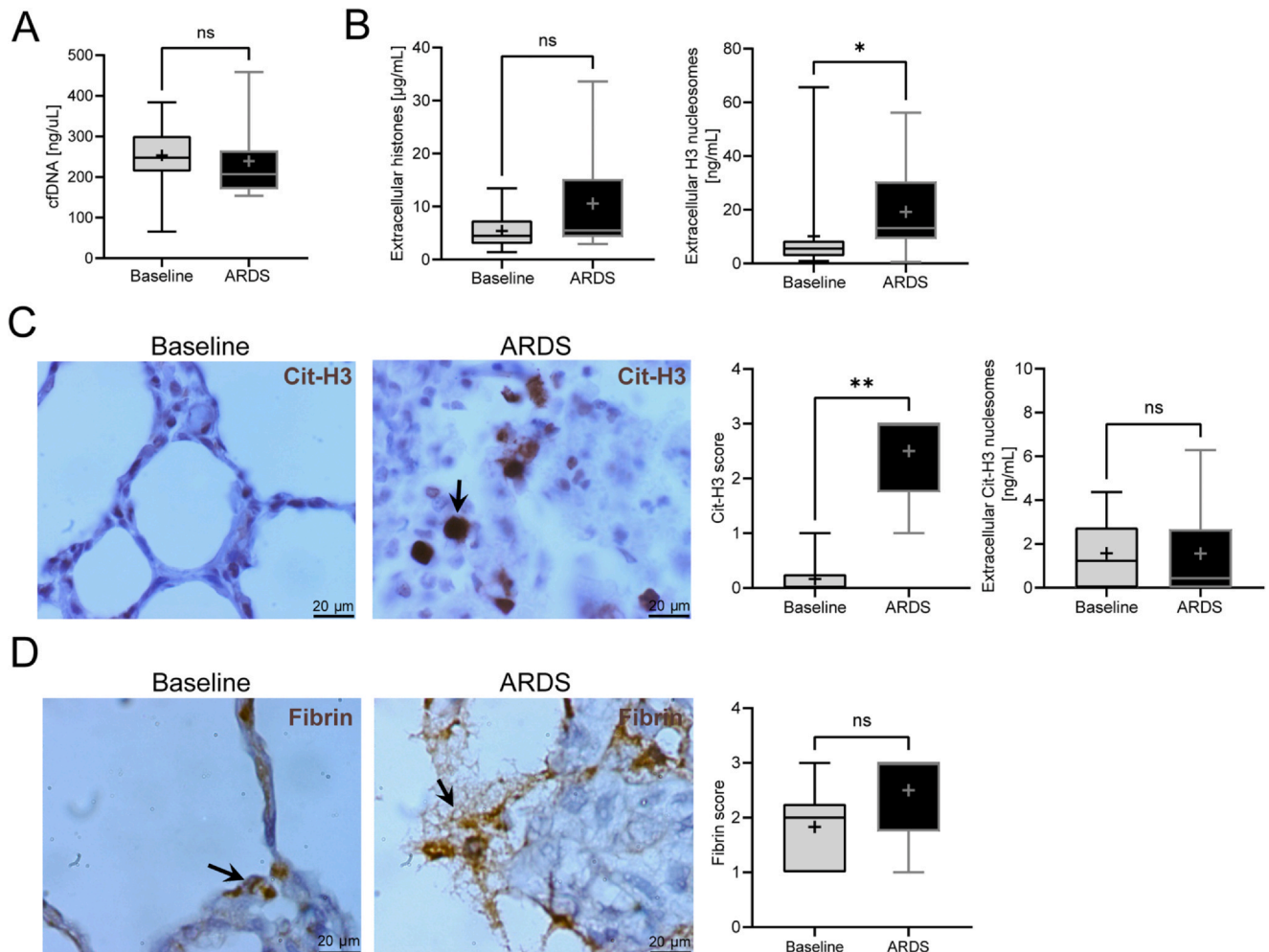


**Figure 3** Molecular analysis of aspiration-induced ARDS showed increased levels of extracellular H3 nucleosomes in plasma and citrullinated H3 in tissue. (A) Levels of cell-free DNA in plasma at baseline and confirmed ARDS ( $n = 12$ ). (B) Total extracellular histone levels in plasma quantified by western blot (left) and extracellular H3 nucleosome levels quantified by (right) at baseline compared to after confirmation of ARDS ( $n = 12$ ). (C) Representative images (left) and quantification ( $n = 6$ ; middle) of citrullinated (Cit)-H3 in tissue identified by immunohistochemistry, indicated by brown staining and black arrow and extracellular Cit-H3 nucleosome levels measured in plasma by ELISA (right,  $n = 12$ ) at baseline compared to after confirmation of ARDS. (D) Fibrin depositions were quantified by immunohistochemistry. Representative images at baseline and after ARDS was confirmed show fibrin depositions in lung tissue (brown indicated by black arrows) quantified with a fibrin score (right,  $n = 6$ ). Scale bars represent 20  $\mu\text{m}$ . Data are presented as boxplots with median lines, a plus at the mean and whiskers indicating minimum and maximum. The 2-sided Mann-Whitney test was used to test for statistical significance,  $*p < 0.05$ ,  $**p < 0.01$ . ARDS, acute respiratory distress syndrome; cfDNA, cell-free DNA; ns, not significant.

(Figure 5G, left and center). Fibrin scores were  $1.83 \pm 1.47$  in the nontreated group and  $0.33 \pm 0.52$  in treated lungs ( $p = 0.1126$ ; Figure 5G, right).

### Identification of immune cells in the grafts after EVLP

To better understand the mechanism and nature of the NET removal and obtain insights into which immune cells might be involved in the process, we performed immunohistochemical staining for allograft inflammatory factor-1 (AIF-1), a marker for monocytes and macrophages (Figure 6A). We compared tissue sections from treated to those from nontreated grafts after 4 hours of EVLP and detected a significantly higher amount of fluorescence units in

the treated ( $96.38 \pm 7.51$ ) versus the nontreated group ( $162.00 \pm 37.58$ ;  $p = 0.0087$ , Figure 6B). On the basis of the significant difference in AIF-1 positive cells in between treatment groups, we performed cytokine analysis of BALF and EVLP perfusate after EVLP. We observed significantly lower levels of cytokines in EVLP perfusate in treated compared to nontreated grafts reaching statistical significance for  $\text{IL-1}\beta$  ( $31.30 \pm 10.67$  pg/ml vs  $214.30 \pm 110.30$  pg/ml, respectively;  $p = 0.0022$ , Figure 6C),  $\text{IL-6}$  ( $183.60 \pm 18.54$  pg/ml vs  $673.30 \pm 140.50$  pg/ml, respectively;  $p = 0.0022$ , Figure 6C), and  $\text{IL-12}$  ( $144.20 \pm 81.09$  pg/ml vs  $582.90 \pm 186.40$  pg/ml, respectively;  $p = 0.0022$ , Figure 6C). No statistically significant difference could be identified in cytokine levels in EVLP perfusate for  $\text{IL-8}$ ,  $\text{IL-10}$ , and  $\text{TNF-}\alpha$  (Figure 6C). Those results were mirrored in BALF from treated versus

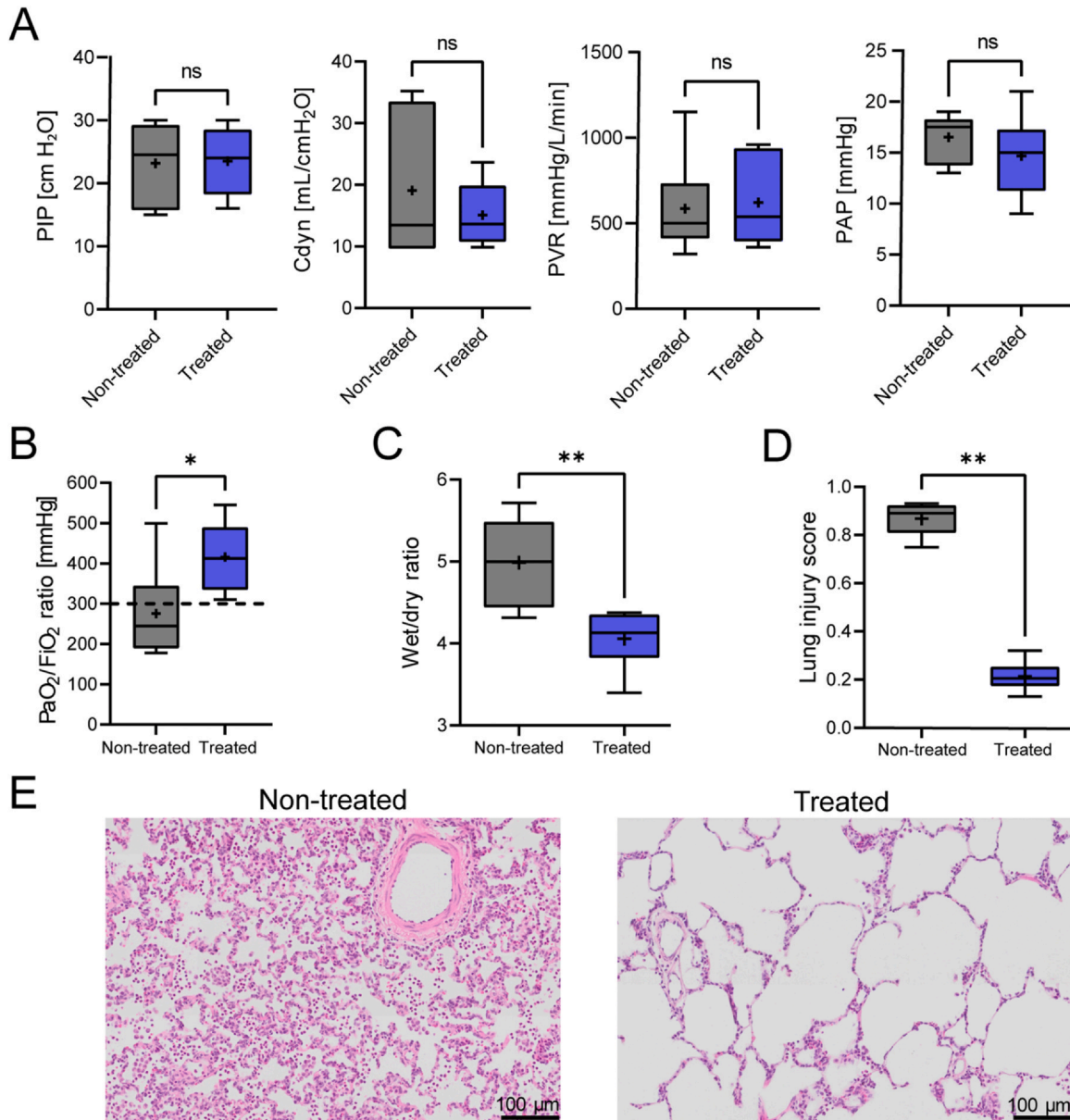


**Figure 4** Ex vivo lung perfusion (EVLV) with neutrophil extracellular trap removal improved hemodynamic parameters and lung morphology. (A) Selected hemodynamic parameters after 4 hours of EVLP comparing lungs that received neutrophil extracellular trap removal treatment (blue,  $n=6$ ) to nontreated lungs (gray,  $n=6$ ), including peak inspiratory pressure, pulmonary vascular resistance, dynamic compliance, and pulmonary artery pressure. (B)  $\text{PaO}_2/\text{FiO}_2$  ratios for treated ( $n=6$ ) and nontreated lungs ( $n=6$ ) after 4 hours of EVLP. The black dotted line at 300 mm Hg indicates the clinical threshold for acceptance of lungs for transplantation. (C) Wet/Dry ratio of lung tissue after 4 hours of EVLP for nontreated and treated lungs ( $n=6$ ). (D) Quantitative lung injury score (right,  $n=6$ ) comparing nontreated versus treated group. (E) Representative images of hematoxylin and eosin-stained histological lung tissue sections of the nontreated (left) versus the treated group (right), where scale bars indicate 100  $\mu\text{m}$ . Data are presented as boxplots with median lines, a plus at the mean, and whiskers indicating minimum and maximum. The 2-sided Mann-Whitney test was used for all statistical analyses, \* $p < 0.05$ , \*\* $p < 0.01$ . Cdyn, dynamic compliance; ns, not significant; PAP, pulmonary artery pressure; PIP, peak inspiratory pressure; PVR, pulmonary vascular resistance.

nontreated grafts with detected lower levels of cytokines for IL-1 $\beta$  ( $1,120 \pm 839.0$  pg/ml vs  $8,080.00 \pm 3,512.00$  pg/ml, respectively;  $p = 0.0022$ , Figure 6D), IL-6 ( $377.40 \pm 138.30$  vs  $985.20 \pm 356.70$  pg/ml, respectively;  $p = 0.0043$ , Figure 6D), and IL-12 ( $212.40 \pm 187.50$  pg/ml vs  $1,167.00 \pm 635.60$  pg/ml, respectively;  $p = 0.0022$ , Figure 6D). Regarding the cytokine levels for IL-8, IL-10, and TNF- $\alpha$  in BALF, no statistically significant difference between treated and nontreated grafts could be detected (Figure 6D).

## Discussion

Removing NETs holds potential as a novel therapeutic strategy for solid organ transplantations. Elevated NET levels have been reported in liver transplantation patients suffering from ischemia-reperfusion injury and are linked to poor outcomes.<sup>29</sup> Furthermore, increased NET levels were reported in kidney transplant recipients, suggesting a broad target group for ex vivo NET removal.<sup>30,31</sup>

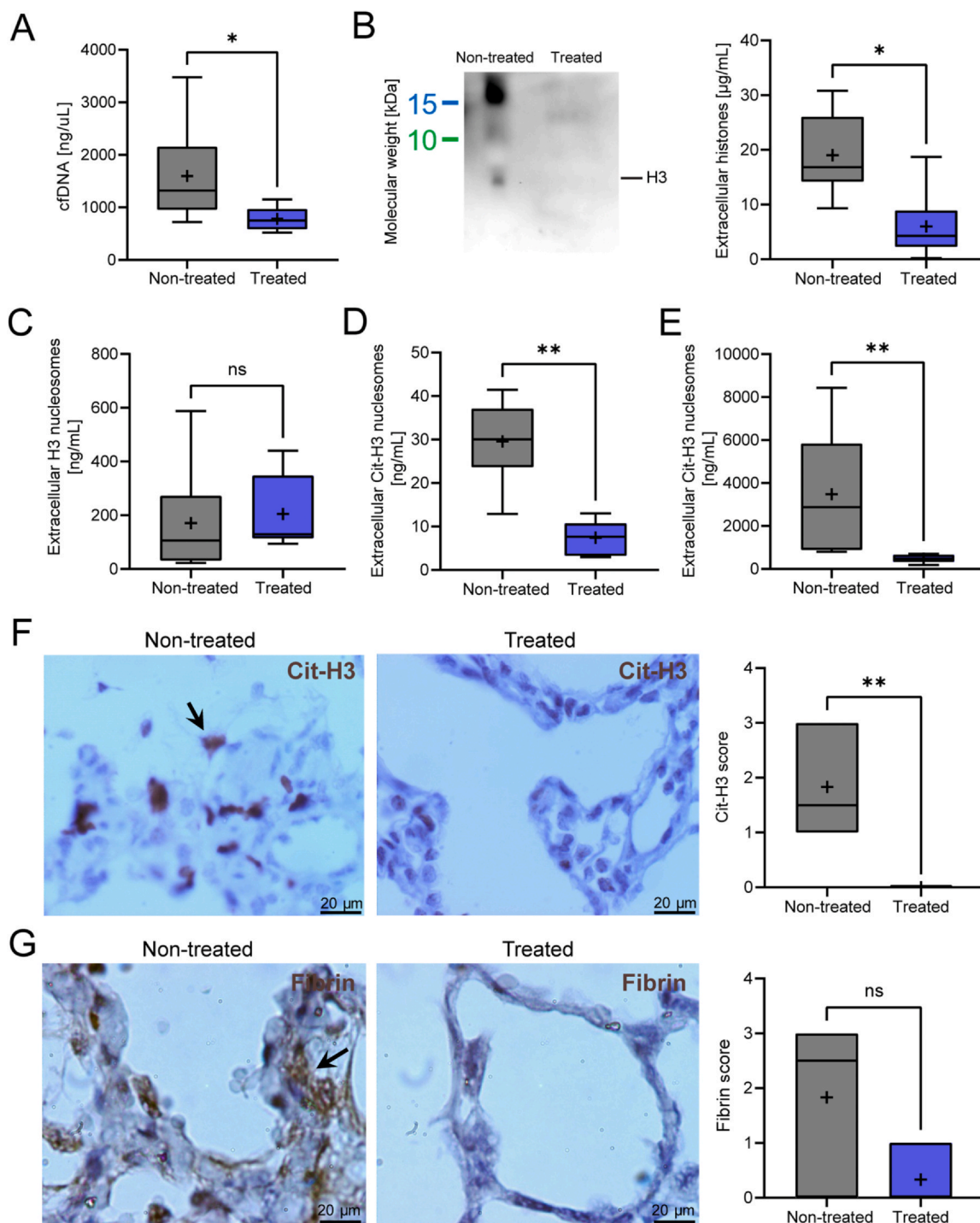


**Figure 5** Neutrophil extracellular trap removal during ex vivo lung perfusion decreases cell-free DNA and other neutrophil extracellular trap-related markers in aspiration-damaged lungs. (A) Levels of cell-free DNA in plasma comparing nontreated and treated lungs ( $n = 6$ ). (B) Total extracellular histone levels in plasma quantified by western blot. Representative image (left) and quantification (right),  $n = 6$ . (C) Extracellular H3 nucleosome levels in plasma were quantified by ELISA ( $n = 6$ ). Levels of extracellular citrullinated (Cit) H3 nucleosomes quantified by ELISA in (D) plasma ( $n = 6$ ) and in (E) bronchoalveolar lavage fluid ( $n = 6$ ) comparing levels of nontreated and treated. (F) Cit-H3 in tissue identified by immunohistochemistry, representative images (left) with Cit-H3 in brown, indicated by a black arrow, scale bars represent 20  $\mu\text{m}$ . Quantitative scoring (right),  $n = 6$ . (G) Fibrin deposition in tissue by immunohistochemistry. Representative images (left), with fibrin visualized in brown. Quantitative scoring (right,  $n = 6$ ). Scale bars represent 20  $\mu\text{m}$ . Data are presented as boxplots with median lines, a plus at the mean, and whiskers indicating minimum and maximum. Two-sided Mann-Whitney tests were used for all statistical analyses,  $*p < 0.05$ ,  $**p < 0.01$ . cfDNA, cell-free DNA; ns, not significant.



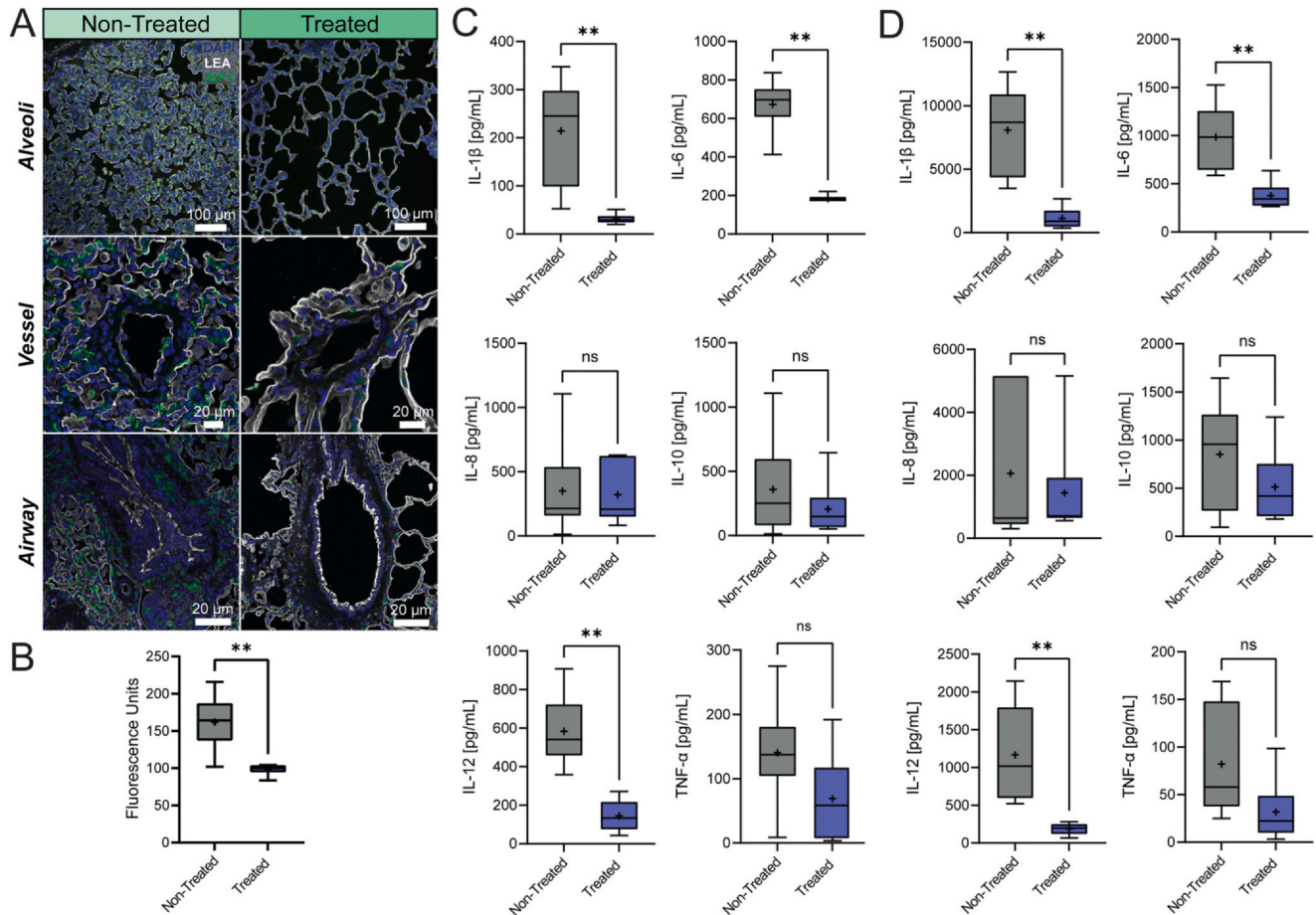


**Figure 6** Immune cell marker AIF-1 and proinflammatory cytokines are decreased in treated versus nontreated grafts after 4 hours of ex vivo lung perfusion (EVLV). (A) Representative images from fluorescent staining of allograft inflammatory factor-1 (in green), 4',6-diamidino-2-phenylindole (in blue), and *Lycopersicon esculentum* lectin (in white) comparing nontreated to treated grafts after 4 hours of EVLP. Scale bars represent 100 and 20  $\mu\text{m}$ , respectively. (B) Quantification of AIF-1 fluorescence units comparing nontreated to treated grafts ( $n = 6$ ). Cytokine levels (C) in EVLP perfusate ( $n = 6$ ) and (D) in bronchoalveolar lavage fluid ( $n = 6$ ), comparing treated to nontreated grafts. Data are presented as boxplots with median lines, a plus at the mean, and whiskers indicating minimum and maximum. Two-sided Mann-Whitney tests were used for all statistical analyses,  $*p < 0.05$ ,  $**p < 0.01$ , and ns = not significant.

Our results demonstrate that combining EVLP and NET removal constitutes a promising therapeutic approach for ameliorating the inflammatory milieu in injured donor lungs. In our porcine model, ARDS was induced by the instillation of intratracheal gastric content and confirmed based on CXR, blood gas analysis, and histology. The levels of NET-specific markers in peripheral blood did not differ pre- and post-ARDS but did in lung tissue, as evidenced by increased Cit-H3 staining. This result is not unexpected, since damage was focused within the lungs. Therefore, it is unlikely that significant levels of NETs, induced within the lung, migrate to the blood during 6 hours of ARDS induction, resulting in elevated NET markers locally but not systemically.

In this study, the combination of EVLP and NET removal enhanced lung function and morphology in injured donor lungs, significantly increasing their oxygenation capacity. Based on improved  $\text{PaO}_2/\text{FiO}_2$  ratios, 5 of 6 lungs surpassed the acceptance threshold for transplantation. A likely explanation is the pathogenicity of NETs in ALIs. Excess NET release causes inflammation and, due to the high content of cytotoxic molecules in NETs, induces

microvascular, cellular and tissue damage, and edema.<sup>13,14,32</sup> Those effects impair gas exchange in the lung, lowering  $\text{PaO}_2/\text{FiO}_2$  ratios. This notion is supported by other studies describing the lung niche as the repository for neutrophils ready to act against invading pathogens.<sup>33</sup> Furthermore, a feed forward mechanism for NETs has been postulated, by which released NETs trigger the release of more NETs leading to amplification and propagation of proinflammatory immune responses.<sup>34</sup> The hypothesis is strengthened by the significant elevation of AIF-1 positive cells and elevated cytokine levels for IL-1 $\beta$ , IL-6, and IL-12, confirming an amplified immune response in the nontreated as compared to the treated lungs. The cytokine levels thus display favorable results for the treated group. All 3 cytokines have previously been shown to be predictive markers of outcome in LTx, which further strengthens the positive effect of the NET removal device.<sup>35-38</sup> Looking into other diseases such as atherosclerosis, NETs have been directly linked to the release of IL-1 $\beta$  from macrophages.<sup>39</sup> Despite more specifically targeted studies being needed in the LTx field to disentangle the net of connections between cytokines and NETs, we propose that removing NETs

prevents damage and improves oxygenation. This is reflected in the higher PaO<sub>2</sub>/FiO<sub>2</sub> ratios after NET removal during EVLP and the parallel decrease in immune cell infiltration and edema. Specifically, the levels of cell-free DNA and extracellular histones by western blot decreased significantly in treated compared with nontreated lungs, consistent with the concomitant decline in extracellular citrullinated H3 nucleosomes. In contrast, extracellular H3 nucleosome levels in plasma did not differ significantly between treated and nontreated lungs, which could be attributed to the potential interfering effects of heparin in the EVLP perfusate. Histones, which form the bulk of the protein content in NETs, provoke inflammatory responses and have been proposed to mediate NET-induced tissue damage in ALI.<sup>14,40-42</sup> Because the NET removal device is predicated on the capture of chromatin using histone-conjugated beads, the improvement in lung function could be attributed to the elimination of histones from circulation.

In regard to the specificity of the device, NET formation can occur through suicidal, vital, or inducible NETosis, generating unique NETs.<sup>32</sup> Our broad-spectrum strategy targets all types of NETs, obviating the need to focus on specific NETosis pathways. While determining the NETosis type in our porcine donor model is interesting, our approach suggests that all NET categories contribute to ARDS pathology and could apply to other NET-mediated lung conditions.

Comparing our approach to other clinically relevant pharmaceuticals such as DNase, DNase dissolves the NET-DNA network but fails to prevent NET-induced tissue damage.<sup>42</sup> This indicates that non-DNA compounds (e.g., histones) in NETs mediate their inflammatory and cytotoxic effects and that therapeutics such as DNase are unlikely to have similar efficacy in this space. In contrast, NET removal eliminates all NET-associated elements, including histones and neutrophil proteins, providing a broad-target, solid-phase-based strategy of inhibiting NETs. This latter property is especially important, because by targeting these chromatin-protein networks, NET removal will not alter cellular function, avoiding medicinal toxicity. Elevated NETs have recently been linked to the development of more severe PGD, negatively impacting the prognosis of lung transplant recipients.<sup>26,27,43</sup> In our study, all lungs exhibited some level of interstitial edema after 4 hours of perfusion, which can favor the development of PGD post-LTx. However, in the analysis of wet-dry ratios, treated lungs showed significantly less edema, which is consistent with a lower risk of PGD.<sup>44</sup> Edema in our model was likely not ischemia-reperfusion injury but rather the induction of aspiration-induced ARDS. As such, the mechanism by which PGD may develop upon transplantation of these lungs might differ from other reports. Notably, previous studies suggested that PGD phenotypes differ between lungs that have undergone ischemia-reperfusion injury and EVLP compared to those that have not.<sup>45</sup> Further, the duration of ischemia can affect PGD phenotype, with longer ischemic times exacerbating severity.<sup>44</sup>

The results of this study are encouraging and provide proof of concept that NET removal has viable therapeutic value in restoring transplantability of previously discarded donor lungs with aspiration-induced ALI. Further studies are necessary to validate our findings, evaluate the

safety and efficacy of EVLP-NET removal in humans, optimize the duration of treatment, and to examine the potential clinical applicability of NET removal post transplantation.

EVLP with NET removal effectively restored pulmonary function in damaged porcine donor lungs, carrying implications for the management of aspiration-induced lung injury and having the potential to broaden the pool of viable donor lungs for transplantation.

## Author contributions

S.L. designed the study. S.L., L.P., G.K., A.A., M.M., and F.O. performed animal experiments. M.M., T.H., and S.L. analyzed clinical data. M.M., J.S., S.T.A., N.B.B., and F.O. performed different parts of the molecular analyses. G.W. and C.H.T. provided supervision and infrastructure in Liverpool. I.C. and M.M. performed histology, M.M., J.S., and G.W. scoring. M.M., F.O., and S.L. acquired data, performed analysis, and prepared the manuscript. All authors read and approved the final version.

## Disclosure statement

A.A. is Chief Medical Officer of SanterSus AG, reflected in the affiliations. The authors declare no competing interests.

The authors thank the Hedenstierna laboratory, Uppsala, Sweden for support during the experiments and Jake Micallef (VolitionRX Limited, Isnes, Belgium) for technical discussions.

The authors gratefully acknowledge funding by the Knut and Alice Wallenberg Foundation, the EU Interreg Öresund-Kattegat-Skagerrak, and grants from the Swedish state under the agreement between the Swedish government and the county councils, the ALF-agreement, and the Swedish research council.

## Data and materials availability

Data and materials are in the main text or supplementary materials and from the corresponding author upon reasonable request.

## Supplementary data

Supplementary data associated with this article can be found in the online version at [doi:10.1016/j.healun.2024.07.007](https://doi.org/10.1016/j.healun.2024.07.007).

## References

1. Perch M, Hayes Jr. D, Cherikh WS, et al. The International Thoracic Organ Transplant Registry of the International Society for Heart and Lung Transplantation: thirty-ninth adult lung transplantation report-

- 2022; focus on lung transplant recipients with chronic obstructive pulmonary disease. *J Heart Lung Transplant* 2022;41:1335-47.
2. Mulvihill MS, Lee HJ, Weber J, et al. Variability in donor organ offer acceptance and lung transplantation survival. *J Heart Lung Transplant* 2020;39:353-62.
  3. Snell GI, Yusef RD, Weill D, et al. Report of the ISHLT Working Group on Primary Lung Graft Dysfunction, part I: definition and grading-A 2016 Consensus Group statement of the International Society for Heart and Lung Transplantation. *J Heart Lung Transplant* 2017;36:1097-103.
  4. Verleden GM, Raghu G, Meyer KC, Glanville AR, Corris P. A new classification system for chronic lung allograft dysfunction. *J Heart Lung Transplant* 2014;33:127-33.
  5. Raghavendran K, Nemzek J, Napolitano LM, Knight PR. Aspiration-induced lung injury. *Crit Care Med* 2011;39:818-26.
  6. Egan TM, Haightcock BE, Lobo J, et al. Donation after circulatory death donors in lung transplantation. *J Thorac Dis* 2021;13:6536-49.
  7. Orens JB, Boehler A, De Perrot M, et al. A review of lung transplant donor acceptability criteria. *J Heart Lung Transplant* 2003;22:1183-200.
  8. Li H, Zhou X, Tan H, et al. Neutrophil extracellular traps contribute to the pathogenesis of acid-aspiration-induced ALI/ARDS. *Oncotarget* 2018;9:1772-84.
  9. Sayah DM, Mallavia B, Liu F, et al. Neutrophil extracellular traps are pathogenic in primary graft dysfunction after lung transplantation. *Am J Respir Crit Care Med* 2015;191:455-63.
  10. Zhang Y, Wen Z, Guan L, et al. Extracellular histones play an inflammatory role in acid aspiration-induced acute respiratory distress syndrome. *Anesthesiology* 2015;122:127-39.
  11. Papayannopoulos V, Metzler KD, Hakkim A, Zychlinsky A. Neutrophil elastase and myeloperoxidase regulate the formation of neutrophil extracellular traps. *J Cell Biol* 2010;191:677-91.
  12. Brinkmann V, Reichard U, Goosmann C, et al. Neutrophil extracellular traps kill bacteria. *Science* 2004;303:1532-5.
  13. Scozzi D, Liao F, Krupnick AS, Kreisel D, Gelman AE. The role of neutrophil extracellular traps in acute lung injury. *Front Immunol* 2022;13:953195.
  14. Abrams ST, Zhang N, Manson J, et al. Circulating histones are mediators of trauma-associated lung injury. *Am J Respir Crit Care Med* 2013;187:160-9.
  15. Alsbani M, Abrams ST, Cheng Z, et al. Reduction of NETosis by targeting CXCR1/2 reduces thrombosis, lung injury, and mortality in experimental human and murine sepsis. *Br J Anaesth* 2022;128:283-93.
  16. Jarrahi A, Khodadadi H, Moore NS, et al. Recombinant human DNase-I improves acute respiratory distress syndrome via neutrophil extracellular trap degradation. *J Thromb Haemost* 2023;21:2473-84. <https://doi.org/10.1016/j.jtha.2023.04.044>. Epub 2023 May 16. PMID: 37196848; PMCID: PMC10185489.
  17. Ngo ATP, Gollomp K. Building a better NET: neutrophil extracellular trap targeted therapeutics in the treatment of infectious and inflammatory disorders. *Res Pract Thromb Haemost* 2022;6:e12808.
  18. Christophorou MA, Castelo-Branco G, Halley-Stott RP, et al. Citrullination regulates pluripotency and histone H1 binding to chromatin. *Nature* 2014;507:104-8.
  19. Lefrançois E, Mallavia B, Zhuo H, Calfee CS, Looney MR. Maladaptive role of neutrophil extracellular traps in pathogen-induced lung injury. *JCI Insight* 2018;3:e98178. <https://doi.org/10.1172/jci.insight.98178>. PMID: 29415887; PMCID: PMC5821185.
  20. Scozzi D, Wang X, Liao F, et al. Neutrophil extracellular trap fragments stimulate innate immune responses that prevent lung transplant tolerance. *Am J Transplant* 2019;19:1011-23.
  21. Ingemansson R, Eyjolfsson A, Mared L, et al. Clinical transplantation of initially rejected donor lungs after reconditioning ex vivo. *Ann Thorac Surg* 2009;87:255-60.
  22. Machuca TN, Cypel M. Ex vivo lung perfusion. *J Thorac Dis* 2014;6:1054-62.
  23. Yeung JC, Krueger T, Yasufuku K, et al. Outcomes after transplantation of lungs preserved for more than 12h: a retrospective study. *Lancet Respir Med* 2017;5:119-24.
  24. Ghaidan H, Stenlo M, Niroomand A, et al. Reduction of primary graft dysfunction using cytokine adsorption during organ preservation and after lung transplantation. *Nat Commun* 2022;13:4173.
  25. Lindstedt S, Hlebowicz J, Koul B, et al. Comparative outcome of double lung transplantation using conventional donor lungs and non-acceptable donor lungs reconditioned ex vivo. *Inter Cardiovasc Thorac Surg* 2011;12:162-5.
  26. Caldarone L, Mariscal A, Sage A, et al. Neutrophil extracellular traps in ex vivo lung perfusion perfusate predict the clinical outcome of lung transplant recipients. *Eur Respir J* 2019;53.
  27. Bonneau S, Landry C, Bégin S, et al. Correlation between Neutrophil Extracellular Traps (NETs) expression and primary graft dysfunction following human lung transplantation. *Cells* 2022;11:3420.
  28. Surkov K. Method and device for purification of blood from circulating cell-free DNA. In: Organization WIP, editor, G01N 33/53 (2006.01), A61M 1/34 (2006.01), A61M 1/36 (2006.01) ed: Santersus SA; 2019.
  29. von Meijenfeldt FA, Stravitz RT, Zhang J, et al. Generation of neutrophil extracellular traps in patients with acute liver failure is associated with poor outcome. *Hepatology* 2022;75:623-33.
  30. Torres-Ruiz J, Villca-Gonzales R, Gómez-Martín D, et al. A potential role of neutrophil extracellular traps (NETs) in kidney acute antibody mediated rejection. *Transplant Immunol* 2020;60:101286.
  31. Scozzi D, Ibrahim M, Menna C, Krupnick AS, Kreisel D, Gelman AE. The role of neutrophils in transplanted organs. *Am J Transplant* 2017;17:328-35.
  32. Papayannopoulos V. Neutrophil extracellular traps in immunity and disease. *Nat Rev Immunol* 2018;18:134-47.
  33. Li W, Terada Y, Tyurina YY, et al. Necroptosis triggers spatially restricted neutrophil-mediated vascular damage during lung ischemia reperfusion injury. *Proc Natl Acad Sci USA* 2022;119:e2111537119.
  34. Dömer D, Walther T, Möller S, Behnen M, Laskay T. Neutrophil extracellular traps activate proinflammatory functions of human neutrophils. *Front Immunol* 2021;12:636954.
  35. Andreasson ASI, Borthwick LA, Gillespie C, et al. The role of interleukin-1 $\beta$  as a predictive biomarker and potential therapeutic target during clinical ex vivo lung perfusion. *J Heart Lung Transplant* 2017;36:985-95.
  36. Meduri GU, Headley S, Kohler G, et al. Persistent elevation of inflammatory cytokines predicts a poor outcome in ARDS. Plasma IL-1 beta and IL-6 levels are consistent and efficient predictors of outcome over time. *Chest* 1995;107:1062-73.
  37. Sage AT, Richard-Greenblatt M, Zhong K, et al. Prediction of donor related lung injury in clinical lung transplantation using a validated ex vivo lung perfusion inflammation score. *J Heart Lung Transplant* 2021;40:687-95.
  38. Meloni F, Vitulo P, Cascina A, et al. Bronchoalveolar lavage cytokine profile in a cohort of lung transplant recipients: a predictive role of interleukin-12 with respect to onset of bronchiolitis obliterans syndrome. *J Heart Lung Transplant* 2004;23:1053-60.
  39. Warnatsch A, Ioannou M, Wang Q, Papayannopoulos V. Neutrophil extracellular traps license macrophages for cytokine production in atherosclerosis. *Science* 2015;349:316-20.
  40. Abrams ST, Zhang N, Dart C, et al. Human CRP defends against the toxicity of circulating histones. *J Immunol* 2013;191:2495-502.
  41. Hoeksema M, van Eijk M, Haagsman HP, Hartshorn KL. Histones as mediators of host defense, inflammation and thrombosis. *Future Microbiol* 2016;11:441-53.
  42. Saffarzadeh M, Juenemann C, Queisser MA, et al. Neutrophil extracellular traps directly induce epithelial and endothelial cell death: a predominant role of histones. *PLoS One* 2012;7:e32366.
  43. Diamond JM, Lee JC, Kawut SM, et al. Clinical risk factors for primary graft dysfunction after lung transplantation. *Am J Respir Crit Care Med* 2013;187:527-34.
  44. Christie JD, Carby M, Bag R, Corris P, Hertz M, Weill D. Report of the ISHLT working group on primary lung graft dysfunction part II: definition. A consensus statement of the International Society for Heart and Lung Transplantation. *J Heart Lung Transplant* 2005;24:1454-9.
  45. Mallea JM, Hartwig MG, Keller CA, et al. Remote ex vivo lung perfusion at a centralized evaluation facility. *J Heart Lung Transplant* 2022;41:1700-11.